A simple method of calculating eigenvalues and resonances in domains with regular ends

Michael Levitin*
Maxwell Institute for Mathematical Sciences
Department of Mathematics
Heriot-Watt University
Riccarton, Edinburgh EH14 4AS, U. K.
email M.Levitin@ma.hw.ac.uk
www.ma.hw.ac.uk/∼levitin/

Marco Marletta†
School of Mathematics
Cardiff University
Senghennydd Road
Cardiff CF24 4AG, U. K.
email MarlettaM@cardiff.ac.uk
http://www.cf.ac.uk/maths/marlettam/

original version November 8, 2006

Abstract

We present a simple new approach to the solution of a wide class of spectral and resonance problems on infinite domains with regular ends, including those found in the study of quantum switches, waveguides, and acoustic scatterers. Our algorithm is part analytical and part numerical and is essentially a combination of four classical approaches (domain decomposition, boundary elements, finite elements and spectral methods) each of which is used in its most natural context.

Keywords: Helmholtz equation, Laplacian, computation of eigenvalues, scattering, resonances, infinite domains, cylindrical ends, quantum switches, waveguides, domain decomposition, Neumann-to-Dirichlet map

2000 Mathematics Subject Classification: 65N25, 35P25, 35P05, 76B15, 78M25

*M.L. was partially supported by the Engineering and Physical Sciences Research Council grant EP/D054621/1
†M.M. was partially supported by the Engineering and Physical Sciences Research Council grant EP/C008324/1

Contents

1 Introduction

We present a simple new approach to the solution of a wide class of spectral and resonance problems on infinite domains with regular ends, including those found in the study of quantum switches, waveguides, and acoustic scatterers. Our algorithm is part analytical and part numerical and is essentially a combination of four classical approaches (domain decomposition, boundary elements, finite elements and spectral methods) each of which is used in its most natural context.

Our method has three main advantages. Firstly, it allows one to exploit existing library software for PDEs to reduce to a minimum the amount of new code which must be written: meshing, choice of basis functions, preconditioning and solution of linear systems can all be delegated to the library code. Secondly, the method is well adapted to handling resonance or scattering problems, where Dirichlet to Neumann (DN) maps must be continued analytically as functions of the spectral parameter. Thirdly, the need to solve boundary value problems for many different choices of the spectral parameter is totally removed.

A brief outline of the solution procedure is as follows. Firstly, the infinite domain on which the problem is posed is decomposed (*domain decomposition*) into a union of a bounded domain and a finite number of infinite regular ends, e.g. cylinders. We need to assume that on each of these ends, the partial differential equation admits separation of variables. The problem can thereby be reduced to a problem on the finite portion of the domain with extra boundary conditions on the interfaces with the attached ends. This problem can be reduced to a problem on the interfaces through the interior 'Neumann-to-Dirichlet' map, whose matrix elements, with respect to a specially chosen basis on the interfaces (*boundary element method*) are calculated in terms of traces of 'mixed' Neumann eigenfunctions from the interior domain (*spectral method*), which is probably the main new idea of this article. The Neumann eigenfunctions are themselves computed by a *finite element method*. The resulting problem on the interface can be solved by finding roots of some monotone functions calculated by solving a generalized matrix eigenproblem of modest size. This is done by elementary means.

Apart from the need to be able to separate variables at infinity, the remaining parts of our approach work for a wide class of problems with minimal restrictions on the PDE coefficients and the boundary conditions. For simplicity of exposition, however, most of this paper is presented for the case of the Helmholtz equation in domains with cylindrical ends, or in domains exterior to an obstacle.

Since the 1960s there has been a lot of important numerical work on the solution of spectral and scattering problems on the sort of domains we consider. Boundary integral and boundary element methods have often been employed — see, e.g., Colton and Kress [CoKr], Brebbia, Telles and Wrobel [BreTeWr] for reviews. Others have considered domain truncation methods coupled with the use of 'non-reflecting' boundary conditions — see, e.g., Hägstrom and Keller [HaKe]; Givoli, Patlashenko and Keller [GiPaKe]. For the particular case of waveguides, special efficient numerical approaches can be found in Aslanyan, Parnovski and Vassiliev [AsPaVa] and in McIver, Linton, McIver and Zhang [McILiMcIZh]; further work will be mentioned in our review of our numerical results. We do not claim that our approach is more numerically efficient than any of these: what is certainly true, however, is that it is much simpler to implement, requiring just a few lines of MATLAB code rather than some serious work by expert programmers.

Some examples of our code are available from the authors' web pages; we encourage the

reader to download, modify, and use it.

2 Geometry

By $\Omega \subset \mathbb{R}^d$, $d \geq 2$ we denote an unbounded connected domain with N non-intersecting cylindrical ends $\mathcal{C}_1^0, \dots, \mathcal{C}_N^0$. Namely, for each $1 \leq n \leq N$ we choose local coordinates $(x, \mathbf{y})$ such that the cylinder $\mathcal{C}_n^0$ is given by

$$\mathcal{C}_n^0 = \{(x, \mathbf{y}) \ : \ \mathbf{y} \in \Gamma_n^0, \ \ x \geq 0\},$$

where Γ_n^0 is the open bounded connected (but not necessarily simply connected) $(d-1)$-dimensional cross-section of $\mathcal{C}_n^0$.

By a domain with cylindrical ends we understand a domain $\Omega \subset \mathbb{R}^d$ such that

$$\Omega = \Omega_0 \sqcup \bigsqcup_{n=1}^{N} \mathcal{C}_n^0 \, .$$

where $\Omega_0 \subset \mathbb{R}^d$ is a connected bounded open set.

Throughout the paper we assume that the boundary $\partial\Omega$ is at least piecewise C^1 smooth and, for simplicity, satisfies both interior and exterior uniform cone conditions (i.e. $\partial\Omega$ does not have any cusps).

3 Spectral problem; boundary conditions; additional notation

We consider, in Ω, the spectral problem

$$-\Delta u = \lambda u \tag{3.1}$$

subject to the boundary conditions

$$Bu := \left(a(\cdot)u + b(\cdot)\frac{\partial u}{\partial n} \right)\Big|_{\partial\Omega} = 0 \, . \tag{3.2}$$

We shall refer to Problem (3.1), (3.2) as "Problem (P)".

We impose the following restrictions on the boundary coefficients $a(\cdot)$ and $b(\cdot)$:

(B_1) a and b are piecewise smooth functions on the boundary $\partial\Omega$;

(B_2) $a(\cdot) \geq 0$, $b(\cdot) \geq 0$, $a(\cdot)^2 + b(\cdot)^2 \equiv 1$;

(B_3) on each connected component of the part $(\frac{1}{2}, \infty) \times \partial\Gamma_n$ of the infinite boundary of each cylindrical end $\mathcal{C}_n^0$ the functions a and b are constant (but the constants are allowed to differ between the cylinders and even between the connected components of the boundary of each cylinder).

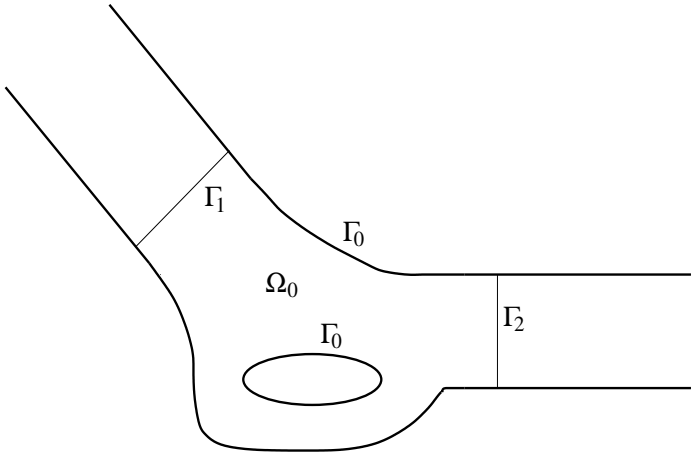

Figure 1: Example of a domain with cylindrical ends.

To finalize our notation, we shall from now on refer to the sets

$$\mathcal{C}_n := \{(x, \mathbf{y}) \ : \ \mathbf{y} \in \Gamma_n^0, \ \ x \geq 1\}$$

and their union

$$\mathcal{C} := \bigsqcup_{n=1}^{N} \mathcal{C}_n$$

as *cylindrical ends* of Ω and the sets

$$\Gamma_n := \{(1, \mathbf{y}) \in \mathcal{C}_n\} = \{(1, \mathbf{y}) \ : \ \mathbf{y} \in \Gamma_n^0\}$$

and their union

$$\Gamma := \bigsqcup_{n=1}^{N} \Gamma_n$$

as *interfaces*.

We also define the *interior part* of Ω as

$$\Omega_0 := \Omega \setminus \mathcal{C}$$

and denote by

$$\Gamma_0 := \partial\Omega_0 \setminus \Gamma \,,$$

the part of its boundary shared with the boundary of Ω.

We emphasize once more that according to (B_3) the boundary condition (3.2) are constant on each connected component of

$$\partial\mathcal{C} \setminus \Gamma = \bigsqcup_{n=1}^{N} (1, \infty) \times \partial\Gamma_n \,.$$

4 Generalized problem

As the reader would easily see later on, all our methods apply, with minimal modifications, to the general second order spectral boundary value problem

$$-\operatorname{div}(p(\cdot)\mathbf{grad}\, u) + q(\cdot)u = \lambda u \tag{4.1}$$

$$(a(\cdot)u + b(\cdot)\mathbf{n}\cdot p(\cdot)\mathbf{grad}\, u(\cdot))|_{\partial\Omega} = 0\,. \tag{4.2}$$

with p being a sufficiently smooth positive definite $(d\times d)$-matrix valued function, and q being an $L_\infty(\mathbb{R}^d)$ scalar potential. Then, in addition to assumptions (B_1)–(B_3), we also require that $p(\cdot)$ and $q(\cdot)$ be constant on each cylindrical end $\mathcal{C}_n^0$ (but the constants are allowed to differ between the cylinders).

Although one can easily formulate all the results and algorithms for the general case (4.1), (4.2), we deliberately describe only Problem (P) for the Laplacian in order to preserve the simplicity and clarity of exposition.

5 Rigorous problem statement

We always understand the spectral problem (P) in the variational sense. Namely, let $\partial_D\Omega := \{\mathbf{x}\in\partial\Omega \ : \ b(\mathbf{x}) = 0\}$ be the part of the boundary on which (3.2) is the Dirichlet condition. Let $C_0^\infty(\Omega) := \{v\in C^\infty(\Omega) \ : \ \overline{\operatorname{supp} v}\cap\partial_D\Omega = \emptyset\}$ be the set of all infinitely differentiable functions on Ω supported away from $\partial_D\Omega$. We define the sesquilinear form

$$\mathfrak{t}[u,v] := \int\limits_\Omega \nabla u\cdot\overline{\nabla v} + \int\limits_{\partial\Omega\setminus\partial_D\Omega} \frac{a}{b}u\overline{v} \tag{5.1}$$

first on $C_0^\infty(\Omega)$, and then extend it to the closure $H^1_*(\Omega)$ of $C_0^\infty(\Omega)$ with respect to the norm associated with (5.1).

From now on, we shall understand Problem (P) as the spectral problem $\mathfrak{t}[u,v] = \lambda\langle u,v\rangle$, where $\langle\cdot,\cdot\rangle$ denotes the scalar product in $L_2(\Omega)$, with the form domain in $H^1_*(\Omega)$. In particular λ is an *eigenvalue* of Problem (P) if there exists a nontrivial function $u\in H^1_*(\Omega)$ such that $\mathfrak{t}(u,v) = \lambda\langle u,v\rangle$ for all $v\in H^1_*(\Omega)$.

6 Known results

The amount of literature published in the last few years on waveguide problems, covering either analytical, numerical or physical aspects, is too big to review adequately here. We mention just a few trends, with our list of references being far from exhaustive.

On a purely mathematical side, attention has recently concentrated on finding conditions sufficient for existence of eigenvalues either below the essential spectrum or embedded in it, see e.g. [EvLeVa, ExSe, DuEx, KrKr]. Additionally, there are some partial results on non-existence of eigenvalues in the lower part of the essential spectrum [DaPa], and on perturbations of embedded eigenvalues which turn them into resonances. On an abstract approach to counting the eigenvalues, see [Par, Ch, ChZw].

Various related numerical methods and applications to a variety of physically motivated special cases and generalisations can be found, e.g., in [Ur, BoJo, HaPaGi, PeJo, Bo] and references therein.

7 Transversal problem and essential spectrum

We need to consider the following *transversal* problem on the joint interface Γ:

$$-\Delta_{d-1} w = \kappa w\,, \qquad \left(a(\cdot)w + b(\cdot)\frac{\partial w}{\partial \nu}\right)\Big|_{\partial\Gamma} = 0\,; \tag{7.1}$$

here Δ_{d-1} is the $(d-1)$-dimensional Laplacian and $\frac{\partial}{\partial \nu}$ is the derivative with respect to the external normal ν to $\partial\Gamma$ (which of course coincides here with the normal n to $\partial\Omega$). We recall that a and b are constant on each connected component of $\partial\Gamma$.

This problem has a rigorous formulation in terms of sesquilinear forms analogous to that introduced in (5.1) but with Ω replaced by Γ throughout. The assumptions (B_1), (B_2) and (B_3) ensure that the problem (7.1) has a purely discrete spectrum of non-negative eigenvalues $(\kappa_j)_{j=1}^{\infty}$, enumerated in increasing order and repeated according to multiplicity; we denote by $(w_j(\mathbf{y}))_{j=1}^{\infty}$ the corresponding eigenfunctions normalized in $L_2(\Gamma)$. We also set $\kappa_0 := -\infty$.

It is well known that the essential spectrum of Problem (P) is then given by $[\kappa_1, +\infty)$ and moreover its multiplicity at a point $\lambda \geq \kappa_1$ is equal to the number of κ_j which are less than or equal to λ. We shall often refer to the number κ_j as the j-th *threshold*.

For each $J \geq 1$ we define

$$P_J := \mathsf{Span}\{w_j \,:\, j > J\}\,,$$

set $P_0 := L_2(\Gamma)$, and denote by $\mathcal{P}_J$ the projection in $L_2(\Gamma)$ onto P_J ($J \geq 0$). We also define $\mathcal{Q}_J := I - \mathcal{P}_J$.

8 Eigenvalue problem — reduction to the interface

We define formally two Neumann to Dirichlet operators, for the interior part Ω_0 and cylindrical ends $\mathcal{C}$.

Firstly, the interior Neumann to Dirichlet operator $\mathcal{R}_\lambda^0 := g \mapsto v|_\Gamma$ is the map which maps any suitable function g defined on Γ to the trace on Γ of the solution of the boundary value problem

$$-\Delta v = \lambda v \ \text{ in } \ \Omega_0, \quad \frac{\partial v}{\partial n} = g \ \text{ on } \ \Gamma, \quad Bv = 0 \ \text{ on } \ \Gamma_0 \tag{8.1}$$

(where by n we always mean the unit normal to Γ directed outwards from Ω_0) provided λ is not an eigenvalue for the corresponding Neumann problem

$$-\Delta U = \lambda U \ \text{ in } \ \Omega_0, \quad \frac{\partial U}{\partial n} = 0 \ \text{ on } \ \Gamma, \quad BU = 0 \ \text{ on } \ \Gamma_0. \tag{8.2}$$

Secondly, the exterior Neumann to Dirichlet operator $\mathcal{R}_\lambda^{\mathcal{C}} := g \mapsto V|_\Gamma$ is the map which maps any suitable function g defined on Γ to the trace on Γ of the solution of the exterior

boundary value problem

$$-\Delta V = \lambda V \text{ in } \mathcal{C}, \quad -\frac{\partial V}{\partial n} = g \text{ on } \Gamma, \quad BV = 0 \text{ on } \partial\mathcal{C} \setminus \Gamma \tag{8.3}$$

(the normal n on Γ, as before, points outwards from Ω_0 along the positive x-axis of each cylindrical end, and therefore towards $\mathcal{C}$).

Suppose that u is an eigenfunction of Problem (P) with eigenvalue λ. It is well known that u is infinitely differentiable at any interior point of Ω. In particular, therefore, u and its gradient restrict to the interface Γ as smooth functions, and so we may define

$$f := u|_\Gamma\,, \quad g = \left.\frac{\partial u}{\partial n}\right|_\Gamma\,. \tag{8.4}$$

Thus f and g satisfy

$$f = -\mathcal{R}^{\mathcal{C}}_\lambda g = \mathcal{R}^0_\lambda g,$$

so that a necessary condition for λ to be an eigenvalue of Problem (P) is that $\sigma = -1$ be an eigenvalue[1] of the operator pencil problem

$$(\sigma\mathcal{R}^{\mathcal{C}}_\lambda - \mathcal{R}^0_\lambda)g = 0\,. \tag{8.5}$$

A graph of a typical behaviour of one of the eigenvalues σ of (8.5) as a function of λ is shown in Fig. 2. In fact, this is one of the eigenvalues of the pencil which arises for a twisted waveguide problem - Example 1 in Section 14.

9 Problem on a cylindrical end — the Neumann to Dirichlet operator

Suppose that V is a solution of the exterior problem (8.3) for some λ (not necessarily an eigenvalue of Problem (P)). A formal expansion of V in terms of the eigenfunctions w_j of the transversal problem (7.1),

$$V(x,\mathbf{y}) = \sum_{j=1}^{\infty} c_j(x) w_j(\mathbf{y})$$

with account of (8.3) yields for the functions c_j the ordinary differential boundary value problems

$$\frac{d^2c_j(x)}{dx^2} + (\lambda - \kappa_j)c_j(x) = 0 \quad \text{for } x > 1\,, \qquad \left.\frac{dc_j(x)}{dx}\right|_{x=1} = -(g, w_j)\,. \tag{9.1}$$

where $(\cdot,\cdot)$ denotes the scalar product in $L_2(\Gamma)$.

The two solutions of (9.1) are

$$c_j^{\pm}(x) = \mp\frac{(g,w_j)}{\sqrt{\kappa_j - \lambda}} \exp\left(\pm(x-1)\sqrt{\kappa_j - \lambda}\right)\,. \tag{9.2}$$

[1] A number σ_0 is called an eigenvalue of a general operator pencil $\sigma A + B$ if zero is an eigenvalue of the operator $\sigma_0 A + B$.

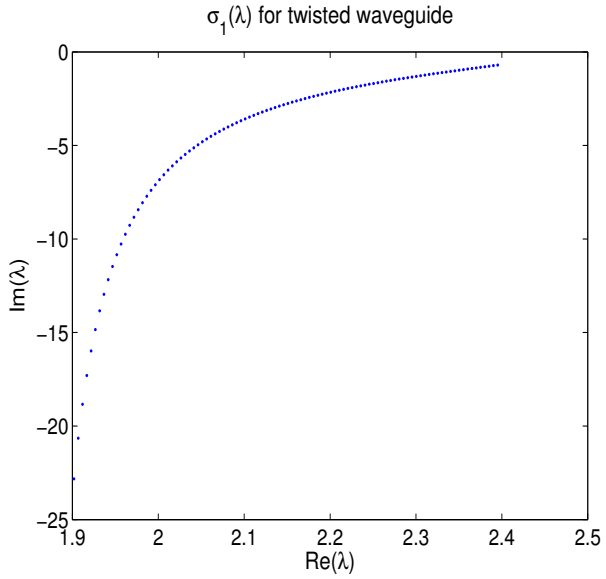

Figure 2: Pencil eigenvalue as a function of λ

If we additionally require that the solution $V \in H^1_*(\mathcal{C})$ and assume that, for some integer $J \geq 0$, $\lambda \in [\kappa_J, \kappa_{J+1})$, then the boundary Neumann data g should belong to the space $\mathcal{Q}_J H_*^{-1/2}(\Gamma)$ (in particular, we need $(g, w_j) = 0$ for $j \leq J$) and choose only the solutions $c_j(x) := c_j^-(x)$ in order to to exclude terms growing or oscillating at $x = +\infty$. Then $V(1, \mathbf{y}) = \sum_{j=J+1}^{\infty} c_j(1) w_j(\mathbf{y}) \in H_*^{1/2}(\Gamma)$ and we have therefore defined the non-negative self-adjoint operators

$$\mathcal{R}^{\mathcal{C}}_{\lambda} : \mathcal{Q}_J H_*^{-1/2}(\Gamma) \to \mathcal{Q}_J H_*^{1/2}(\Gamma) \quad \text{for } \lambda \in [\kappa_J, \kappa_{J+1})$$

acting as

$$\mathcal{R}^{\mathcal{C}}_{\lambda} g = \sum_{j=J+1}^{\infty} \frac{1}{\sqrt{\kappa_j - \lambda}} (g, w_j) w_j. \tag{9.3}$$

It is clear from (9.3) and from the construction that the quadratic form $(\mathcal{R}^{\mathcal{C}}_{\lambda} g, g)_{\Gamma}$ is monotone increasing in λ on each interval $[\kappa_J, \kappa_{J+1})$.

10 Problem on an interior domain — the Neumann to Dirichlet operator

Let g_1 and g_2 be functions defined on Γ and suppose that v_1 and v_2 are the corresponding solutions of the boundary value problem (8.1), for λ which is not an eigenvalue of (8.2). A formal integration by parts shows that

$$(\mathcal{R}^0_{\lambda} g_1, g_2) = (g_1, \mathcal{R}^0_{\lambda} g_2) = \langle \nabla v_1, \nabla v_2 \rangle - \lambda \langle v_1, v_2 \rangle \,. \tag{10.1}$$

This allows us to define a quadratic form

$$\mathfrak{r}_\lambda[g] := (\mathcal{R}^0_\lambda g, g) = \langle \nabla v, \nabla v\rangle - \lambda\langle v, v\rangle$$

(where v solves (8.1)) associated with $\mathcal{R}^0_\lambda$ and hence to regard $\mathcal{R}^0_\lambda$ either as a self-adjoint operator on a domain in $L_2(\Gamma)$ or, under suitable smoothness restrictions on the boundary $\partial\Omega_0$, as a map on a scale of Sobolev spaces from $H^{s-1/2}(\Gamma)$ to $H^{s+1/2}(\Gamma)$ (see [Ag, Pal, Sa]). We emphasize that we impose a condition that λ is not an eigenvalue of (8.2) — for ways of bypassing this condition see [Sa].

For a fixed $g \in L_2(\Gamma)$, the form $\mathfrak{r}_\lambda[g]$ is known to be monotone increasing with respect to λ in any interval not containing the eigenvalues of (8.2), as the following simple argument (found e.g. in [Fr]) shows. Let g be fixed and let v' denote the derivative with respect to λ of the solution v of (8.1). Then v' solves the boundary value problem

$$-\Delta v' = \lambda v' + v \quad \text{in } \Omega_0\,, \quad \partial v'/\partial n|_\Gamma = 0\,, \quad Bv'|_{\Gamma_0} = 0\,. \tag{10.2}$$

Multiplying (10.2) by $\overline{v'}$ and integrating by parts we obtain

$$\frac{1}{2}\,\frac{d}{d\lambda}\mathfrak{r}_\lambda[g] = \left(\frac{d}{d\lambda}(\mathcal{R}^0_\lambda g), g\right)_\Gamma = \left(v', \frac{\partial v}{\partial \nu}\right)_\Gamma = \langle v, v\rangle_{\Omega_0} \geq 0, \tag{10.3}$$

which proves the claim. Exactly the same argument can be used to prove the monotonicity in λ of the form of the operator $\mathcal{R}^{\mathcal{C}}_\lambda$, which we established at the end of the previous section by direct inspection of (9.3).

11 Problem on an interior domain — basis expansions

In section 9, we constructed an explicit representation (9.3) for the Neumann to Dirichlet operator $\mathcal{R}^{\mathcal{C}}_\lambda$ associated with the problem on a cylindrical end. The aim of this section is to do the same for the *interior* Neumann to Dirichlet map $\mathcal{R}^0_\lambda$, and we want to emphasize that the following trick is in fact the focal point of this paper.

In the setting of problem (8.1), let us choose an *arbitrary* basis $\{\phi_k\}_{k=1}^\infty$ in $L_2(\Gamma)$ (which is the domain of the quadratic form $\mathfrak{r}_\lambda$). Let us also denote by Φ_k the solution v of (8.1) with $g = \phi_k$, i.e. of

$$-\Delta\Phi_k = \lambda\Phi_k \ \text{ in } \ \Omega_0, \quad \frac{\partial\Phi_k}{\partial n} = \phi_k \ \text{ on } \ \Gamma, \quad B\Phi_k = 0 \ \text{ on } \ \Gamma_0. \tag{11.1}$$

We also denote by μ_m the eigenvalues and by U_m the corresponding eigenfunctions of the homogeneous problem (8.2), i.e.

$$-\Delta U_m = \mu_m U_m \ \text{ in } \ \Omega_0, \quad \frac{\partial U_m}{\partial n} = 0 \ \text{ on } \ \Gamma, \quad BU_m = 0 \ \text{ on } \ \Gamma_0, \tag{11.2}$$

Our aim is to find explicit expressions for the matrix elements $R_{k\ell} := (\mathcal{R}^0_\lambda\phi_k, \phi_\ell)_\Gamma$.

By (10.1) we have

$$R_{k\ell} = (\mathcal{R}^0_\lambda\phi_k, \phi_\ell)_\Gamma = \langle\nabla\Phi_k, \nabla\Phi_\ell\rangle - \lambda\langle\Phi_k, \Phi_\ell\rangle\,. \tag{11.3}$$

We now use the fact that the eigenfunctions U_m form a basis in the Hilbert space $H^1_*(\Omega_0)$. We can thus expand Φ_k in this basis as

$$\Phi_k = \sum_{m=1}^{\infty} U_m \langle \Phi_k, U_m \rangle \, .$$

Thus we get, expanding the right-hand side of (11.3) with the use of two elementary integrations by parts,

$$\begin{aligned} R_{k\ell} &= \sum_{m=1}^{\infty} \langle \nabla U_m, \nabla U_m \rangle \langle \Phi_k, U_m \rangle \langle U_m, \Phi_\ell \rangle \\ &= \sum_{m=1}^{\infty} (\mu_m - \lambda) \langle \Phi_k, U_m \rangle \langle U_m, \Phi_\ell \rangle = \sum_{m=1}^{\infty} \frac{1}{\mu_m - \lambda} (\phi_k, U_m|_\Gamma)_\Gamma \cdot (U_m|_\Gamma, \phi_\ell)_\Gamma \, . \end{aligned} \tag{11.4}$$

12 Embedded eigenvalues and orthogonality conditions

We have already established formally in section 8 that if λ is an eigenvalue of Problem (P) then $\sigma = -1$ is an eigenvalue of the eigenvalue pencil problem (8.5) on the interface Γ. In view of rigorous definitions of the exterior Neumann to Dirichlet operator, we want now to consider, for $\lambda \in [\kappa_J, \kappa_{J+1})$, the pencil

$$\mathcal{A}_\lambda(\sigma) := \sigma \mathcal{R}^{\mathcal{C}}_\lambda - \mathcal{Q}_J \mathcal{R}^0_\lambda \, . \tag{12.1}$$

acting in a weak sense in $\mathcal{Q}_J L_2(\Omega)$.

For each fixed λ (which plays a role of a parameter rather than spectral parameter) $\mathcal{A}_\lambda(\sigma)$ has σ-spectrum $\mathrm{spec}(\mathcal{A}_\lambda)$, and a necessary condition for λ to be an eigenvalue of Problem (P) is that $-1 \in \mathrm{spec}(\mathcal{A}_\lambda)$. The corresponding eigenfunction $g \in \mathcal{Q}_J L_2(\Gamma)$ is the normal derivative on Γ of the eigenfunction u of Problem (P) corresponding to λ. Also, if $\lambda \in [\kappa_J, \kappa_{J+1})$ for some $J > 0$ then we have seen in section 9 that g must additionally satisfy the orthogonality condition $\mathcal{P}_J \mathcal{R}^0_\lambda g = (I - \mathcal{Q}_J)\mathcal{R}^0_\lambda g = 0$; in other words $\mathcal{R}^0_\lambda g \in \mathcal{Q}_J L_2(\Omega)$.

Since $\mathcal{Q}_J L_2(\Omega)$ is an invariant space of the operator $\mathcal{R}^{\mathcal{C}}_\lambda$, we propose the following strategy for finding embedded eigenvalues:

- first find those "suspicious points" λ_* for which $\sigma = -1$ is an eigenvalue of the operator pencil (12.1) on the interface Γ;
- if these "suspicious" λ_* lie in $[\kappa_J, \kappa_{J+1})$ for some $J > 0$, check the orthogonality condition $\mathcal{P}_J \mathcal{R}^0_{\lambda_*} g = 0$ for the corresponding pencil eigenfunction $g \in \mathcal{Q}_J L_2(\Gamma)$.

Assume that we wish to find the eigenvalues in the interval $[\kappa_J, \kappa_{J+1})$. We start by reducing the spectral problem for the pencil (12.1) on the space $\mathcal{Q}_J L_2(\Gamma)$ to a spectral problem for an infinite matrix pencil. In section 9 we developed a representation of the operator $\mathcal{R}^{\mathcal{C}}_\lambda$ in terms of the transverse eigenfunctions w_j; in section 11 we developed a representation for $\mathcal{R}^0_\lambda$ in terms of an arbitrary basis $\{\phi_k\}_{k=1}^\infty$ in $L_2(\Gamma)$. We now choose as our basis of $\mathcal{Q}_J L_2(\Gamma)$ the set $\{\phi_k\}_{k=1}^\infty$ given by $\phi_k = w_{k+J}$, $k \in \mathbb{N}$. Consequently we obtain from (11.4)

$$R_{k\ell} := (\mathcal{R}^0_\lambda w_{k+J}, w_{\ell+J})_\Gamma = \sum_{m=1}^{\infty} \frac{1}{\mu_m - \lambda} (w_{k+J}, U_m|_\Gamma)_\Gamma \cdot (U_m|_\Gamma, w_{\ell+J})_\Gamma . \tag{12.2}$$

We simplify the expression for the infinite matrix $\mathsf{R}(\lambda) = (R_{k\ell})_{1\le k,\ell<\infty}$ by introducing some notation. Define an infinite matrix S with entries $(S_{km})_{1\le k,m<\infty}$ defined by

$$S_{km} = (w_k, U_m|_\Gamma)_\Gamma\,, \tag{12.3}$$

an infinite diagonal matrix $\mathsf{D}(\lambda)$ with diagonal entries

$$D_{kk}(\lambda) = (\mu_k - \lambda)^{-1}, \quad 1 \le k < \infty, \tag{12.4}$$

and an infinite diagonal matrix $\mathsf{T}(\lambda)$ with diagonal entries

$$T_{kk}(\lambda) = \frac{1}{\sqrt{\kappa_k - \lambda}}, \quad 1 \le k < \infty. \tag{12.5}$$

For a general matrix M we will use the notation $M_{a:b,c:d}$ to denote the submatrix

$$(M_{ij})_{\substack{a\le i\le b\\ c\le j\le d}}\,, \tag{12.6}$$

where $b = \infty$ and $d = \infty$ are allowed.

The matrix R whose entries are defined in (12.2) can now be written as

$$\mathsf{R}(\lambda) = \mathsf{S}_{J+1:\infty,1:\infty}\mathsf{D}(\lambda)\,(\mathsf{S}_{J+1:\infty,1:\infty})^*\,. \tag{12.7}$$

In a similar way, we can define the matrix elements associated with $\mathcal{R}^{\mathcal{C}}_\lambda$ with respect to the same basis using (9.3): $\mathcal{R}^{\mathcal{C}}_\lambda$ has a diagonal matrix representation $\mathsf{T}(\lambda)$ in this basis. We thus obtain the following reduction of the problem from $\mathcal{Q}_J L_2(\Gamma)$ to $\ell^2(\mathbb{N})$.

Theorem 12.1. *A number $\lambda \in [\kappa_J, \kappa_{J+1})$ (which is assumed not to be an eigenvalue of the auxilliary Neumann problem* (11.2)*) is an eigenvalue of Problem (P) if and only if -1 is a σ-eigenvalue of the matrix pencil*

$$\sigma\mathsf{R}(\lambda) - \mathsf{T}(\lambda) \equiv \sigma\mathsf{S}_{J+1:\infty,1:\infty}\mathsf{D}(\lambda)\,(\mathsf{S}_{J+1:\infty,1:\infty})^* - \mathsf{T}(\lambda)\,, \tag{12.8}$$

and, if $J > 0$, the correspoding eigenvector c *of* (12.8) *satisfies the orthogonality condition*

$$\mathsf{S}_{1:J,1:\infty}\mathsf{D}(\lambda)\,(\mathsf{S}_{J+1:\infty,1:\infty})^*\,\mathsf{c} = 0. \tag{12.9}$$

Proof. Let $\lambda \in [\kappa_J, \kappa_{J+1})$ be an eigenvalue of Problem (P), let $u(x, \mathbf{y}) \in H^1_*(\Omega)$ be a corresponding eigenfunction, and let its traces f and g be defined by (8.4). Then the restriction of u to the cylindrical ends $\mathcal{C}$ is a square integrable solution of (3.1) and therefore $\mathcal{P}_J f = \mathcal{P}_J g = 0$ (or $\mathcal{Q}_J g = g$) and $-\mathcal{R}^{\mathcal{C}}_\lambda g = -\mathcal{R}^{\mathcal{C}}_\lambda \mathcal{Q}_J g = f$, with $\mathcal{RC}_\lambda$ given by (9.3). Similarly, from the restriction on the interior part Ω_0, we obtain that $f = \mathcal{R}^0_\lambda g$ which immediately leads to

$$\mathcal{A}_\lambda(-1)g = (-\mathcal{R}^{\mathcal{C}}_\lambda - \mathcal{Q}_J\mathcal{R}^0_\lambda)g = 0 \tag{12.10}$$

and additionally implies the orthogonality condition

$$\mathcal{P}_J\mathcal{R}^0_\lambda g = 0\,. \tag{12.11}$$

If we now write $g = \sum_{k=1}^\infty \mathsf{c}_k w_{k+J}$ with $\mathsf{c}_k = (g, w_{k+J})_\Gamma$ and use the definitions (12.2)–(12.7), then by elementary matrix manipulations (12.10) turns into $(-\mathsf{R}(\lambda) - \mathsf{T}(\lambda))\mathsf{c} = 0$ and (12.11) becomes (12.9). □

13 More on eigenvalues of the operator pencil (12.1)

Before we proceed to descrtibing in detail the numerical procedure which implements Theorem 12.1, we want to establish some more facts about the eigenvalues $\sigma_j(\lambda)$ of the operator pencil $\mathcal{A}_\lambda(\sigma) = \sigma\mathcal{R}^{\mathcal{C}}_\lambda - \mathcal{Q}_J\mathcal{R}^0_\lambda$ (for $\lambda \in [\kappa_J, \kappa_{J+1})$). We enumerate the pencil eigenvalues $\sigma_j(\lambda)$ in decreasing order: $\sigma_1(\lambda) \geq \sigma_2(\lambda) \geq \dots$.

Lemma 13.1. *The σ-eigenvalues of $\mathcal{A}_\lambda(\sigma)$ are monotone increasing functions of λ on each interval $[\Lambda_1, \Lambda_2] \subset [\kappa_J, \kappa_{J+1})$ which does not contain any eigenvalues μ_m of the homogeneous Neumann problem* (11.2).

Proof. We have already established in sections 9 and 10 that each of the operators $\mathcal{R}^{\mathcal{C}}_\lambda$ and $\mathcal{Q}_J\mathcal{R}^0_\lambda$ is monotone increasing (in the sense of corrresponding forms) on each interval satisfying the conditions of the Lemma. Thus, for each fixed negative value of σ, the quadratic form of the pencil $\mathcal{A}_\lambda(\sigma)$ is monotone decresing in λ, and, as $\mathcal{R}^{\mathcal{C}}_\lambda > 0$, by the inverse function theorem the eigenvalues $\sigma(\lambda)$ increase as functions of λ. □

We also want to estimate how many pencil eigenvalue curves $\sigma(\lambda)$ can cross the line $\sigma = -1$ as λ increases in a given interval (or, which is the same, to estimate *a priori* how many eigenvalues of Problem (P) can be located in a given interval). We need to introduce some additional notation. Let ν_m denote the eigenvalues of the interior homogeneous Dirichlet problem:

$$-\Delta U = \nu U \text{ in } \Omega_0, \quad U = 0 \text{ on } \Gamma, \quad BU = 0 \text{ on } \Gamma_0. \tag{13.1}$$

(This problem is similar to (11.2) with the only difference being that an auxilliary Neumann condition on Γ is replaced by the Dirichlet one.).

Lemma 13.2. *Let $\Lambda_2 \in (\kappa_J, \kappa_{J+1}) \setminus \{\mu_m\}$, and let $\Lambda_1 > \max\{\kappa_J, \max\{\mu_m : \mu_m < \Lambda_2\}\}$. (In other words, we choose an interval $[\Lambda_1, \Lambda_2]$ in such a manner that it does not contain any thresholds or any Neumann eigenvalues μ_m.) Then the number of eigenvalues of Problem (P) in the interval $[\Lambda_1, \Lambda_2]$ does not exceed*

$$K := \#\{m : \mu_m < \Lambda_2\} - \#\{m : \nu_m < \Lambda_2\}\,. \tag{13.2}$$

Proof. By Lemma 13.1, the curves $\sigma_j(\lambda)$ are monotone in $\lambda \in [\Lambda_1, \Lambda_2]$. We wish to estimate from above the total possible number of times these curves intersect the straight line $\sigma = -1$. Obviously, this does not exceed the number of curves which are above -1 at the right-hand side of the interval $[\Lambda_1, \Lambda_2]$, namely $K' = \#\{j : -1 < \sigma_j(\Lambda_2)\}$. We shall now show that $K' \leq K$, where K is given by (13.2).

Note that any $\lambda_\star$ for which a particular curve $\sigma_j(\lambda)$ crosses $\sigma = -1$ is at the same time characterised by the fact that zero is in the spectrum of the operator $\mathcal{A}_{\lambda_\star}(-1) \equiv -\mathcal{R}^{\mathcal{C}}_{\lambda_\star} - \mathcal{Q}_J\mathcal{R}^{\mathcal{C}}_{\lambda\star}$. Thus,

$$\begin{aligned} K' &\leq \#\{\text{positive eigenvalues of } -\mathcal{R}^{\mathcal{C}}_{\Lambda_2} - \mathcal{Q}_J\mathcal{R}^0_{\Lambda_2}\} \\ &= \#\{\text{negative eigenvalues of } \mathcal{R}^{\mathcal{C}}_{\Lambda_2} + \mathcal{Q}_J\mathcal{R}^0_{\Lambda_2}\}\,. \end{aligned} \tag{13.3}$$

Since $\mathcal{R}^{\mathcal{C}}_\lambda$ is non-negative for any λ, we can majorize the right-hand side of (13.3) by omitting it there (and also dropping the projector $\mathcal{Q}_J$). Thus,

$$K' \leq \#\{\text{negative eigenvalues of } \mathcal{R}^0_{\Lambda_2}\}\,. \tag{13.4}$$

But by [Sa] (which is in turn a generalisation of [Fr], see also [Ag]) there is a known relation between the number of negative eigenvalues of an interior Neumann-to-Dirichlet operator, and the differences of the Neumann and Dirichlet counting functions:

$$\#\{\text{negative eigenvalues of } \mathcal{R}^0_{\Lambda_2}\} = \#\{m : \mu_m < \Lambda_2\} - \#\{m : \nu_m < \Lambda_2\} = K\,. \tag{13.5}$$

□

Remark 13.3. The reader may notice that the estimate (13.2) does not in fact use Λ_1 and is therefore just an estimate on the counting function of the eigenvalues of Problem (P). One can easily improve it if one knowns an estimate from below on the number of negative eigenvalues of the operator $\mathcal{R}^{\mathcal{C}}_{\Lambda_1} + \mathcal{Q}_J\mathcal{R}^0_{\Lambda_1}$, say

$$\#\{\text{negative eigenvalues of } \mathcal{R}^{\mathcal{C}}_{\Lambda_1} + \mathcal{Q}_J\mathcal{R}^0_{\Lambda_1}\} \geq K_1$$

(e.g. obtained numerically). Then in the statement of Lemma 13.2 one can replace K by $K - K_1$. Further improvements are also possible by introducing the counting functions of a generalised Neumann problem instead of the ordinary Neumann problem, but we do not discuss them here.

14 Numerical algorithm

Theorem 12.1 gives the characterisation of the eigenvalues of Problem (P) which forms the basis of our simple numerical approach to their calculation. We emphasize that this approach depends only on having software capable of the following:

- finding eigenvalues and eigenfunctions for problems on bounded domains with mixed boundary conditions (e.g. MATLAB PDE Toolbox, FEMLAB);
- performing quadratures on boundaries and cross-sections of domains;
- finding the first few eigenvalues of a matrix pencil;
- finding the zeros of a monotone real-valued function of a real variable.

Our algorithm in its basic form is as follows:

Main Algorithm.

1. *Truncate the Neumann expansion* (12.2)*: this is formally equivalent to replacing '∞' by some fixed $N \in \mathbb{N}$ in* (12.2)*.*
2. *Calculate numerical approximations to the first N Neumann eigenvalues $(\mu_m)_{m=1}^N$ and their eigenfunctions $(U_m)_{m=1}^N$ for the inner Neumann problem* (8.2)*.*
3. *Choose $M \in \mathbb{N}$ such that the traces of the eigenfunctions $(U_m)_{m=1}^N$ on the interface Γ are well approximated by linear combinations of the first M eigenfunctions $(w_j)_{j=1}^M$ of the interface problem* (7.1)*.*

4. *Calculate the first M eigenvalues $(\kappa_j)_{j=1}^M$ and eigenfunctions $(w_j)_{j=1}^M$ of the interface problem* (7.1) *- either analytically, as in the case of the two-dimensional examples treated here, or numerically in the case of general higher-dimensional examples.*

5. *Calculate the numbers S_{km} in* (12.3) *for $k = 1, \dots, M$, $m = 1, \dots, N$: in other words, truncate the infinite matrix* S *to its leading $M \times N$ submatrix.*

6. *Similarly, calculate the leading $N \times N$ submatix of* $\mathsf{D}(\lambda)$ *and the leading $M \times M$ submatrix of* $\mathsf{T}(\lambda)$.

7. *Fix J, $0 \le J \ll M$ – we shall look for eigenvalues $\lambda \in [\kappa_J, \kappa_{J+1})$.*

8. *Replace the matrix pencil eigenproblem* (12.8) *by the approximation*

$$\sigma \mathsf{S}_{J+1:M,1:N} \mathsf{D}_{1:N,1:N}(\lambda) \left(\mathsf{S}_{J+1:M,1:N}\right)^* - \mathsf{T}_{J+1:M,J+1:M}(\lambda). \tag{14.1}$$

Denote the σ-eigenvalues of this pencil by

$$\sigma_1(\lambda) \ge \sigma_2(\lambda) \ge \dots \ge \sigma_{M-J}(\lambda).$$

9. *Calculate the first N Dirichlet eigenvalues of the problem* (13.1) *and use the estimates of section 13 to obtain an upper bound K on the number of eigenvalues of Problem (P) in $[\kappa_J, \kappa_{J+1})$. Note: $K \ll M$.*

10. *By numerical rootfinding, solve (if possible) the K nonlinear equations*

$$\sigma_j(\lambda) = -1, \quad j = 1, \dots, K. \tag{14.2}$$

Note that care has to be taken if any of the interior Neumann eigenvalues μ_m lies in $[\kappa_J, \kappa_{J+1})$. Away from the μ_m, the σ_j are monotone functions of λ and so the rootfinding is, in principle, easy.

11. *Denote by $\lambda_{j,J}$ the solution of* (14.2) *and by $\mathsf{c}_{j,J}$ the eigenvector of the pencil* (14.1) *with $\lambda = \lambda_{j,J}$, $\sigma = -1$. Check the orthogonality conditions*

$$\mathsf{S}_{1:J,1:N} \mathsf{D}_{1:N,1:N}(\lambda) \left(S_{J+1:M,1:N}\right)^* \mathsf{c}_{j,J} = 0. \tag{14.3}$$

(Of course, these can never be checked exactly: at most one can check that they are 'almost' satisfied and that there is therefore either an embedded eigenvalue or a point of spectral concentration near $\lambda_{j,J}$.)

□

In the absence of error from the numerical approximation of the eigenvalues and eigenfunctions, the accuracy of this algorithm is determined by the choice of N at the very first step. (The choice of M in step 3 is generally less problematic as the transversal eigenfunctions provide rapidly converging approximations to smooth functions on the interface.) N is the number of terms at which the sum in the expression (11.4) for $R_{k\ell}(\lambda)$ is truncated, and unfortunately

this series can be rather slowly convergent. We accelerate the convergence with a cheap trick. Suppose that for some fixed λ_0 we already know $R_{k\ell}(\lambda_0)$. Then (11.4) yields

$$R_{k\ell}(\lambda) - R_{k\ell}(\lambda_0) = \sum_{m=1}^{\infty} \frac{\lambda - \lambda_0}{(\mu_m - \lambda)(\mu_m - \lambda_0)} (\phi_k, U_m|_\Gamma)_\Gamma \cdot (U_m|_\Gamma, \phi_\ell)_\Gamma \,. \tag{14.4}$$

The series in (14.4) converges much more rapidly than the series in (11.4). Moreover the numbers $R_{k\ell}(\lambda_0)$ are easily calculated from (11.3) (with $\lambda = \lambda_0$) by solving the boundary value problems (11.1) numerically (for $\lambda = \lambda_0$) using any reasonable discretization scheme for elliptic PDEs. Our Main Algorithm is then modified by replacing steps 8 and 11 as follows:

8'. Let R^0 denote the matrix with entries $R_{k\ell}(\lambda_0)$ defined in (12.2) (with λ replaced by λ_0. Then the matrix pencil (14.1) is replaced by

(14.5)

$$\sigma \left[\mathsf{R}^0_{J+1:M,J+1:M} + \mathsf{S}_{J+1:M,1:N} \left\{\mathsf{D}_{1:N,1:N}(\lambda) - \mathsf{D}_{1:N,1:N}(\lambda_0)\right\} \left(\mathsf{S}_{J+1:M,1:N}\right)^*\right] - \mathsf{T}_{J+1:M,J+1:M}(\lambda).$$

11'. The orthogonality condition (14.3) is replaced by

$$\left[\mathsf{R}^0_{1-J:0,1:N} + \mathsf{S}_{1:J,1:N} \left\{\mathsf{D}_{1:N,1:N}(\lambda) - \mathsf{D}_{1:N,1:N}(\lambda_0)\right\} \left(S_{J+1:M,1:N}\right)^*\right] \mathsf{c}_{j,J} = 0. \tag{14.6}$$

Note that $\mathsf{R}^0_{1-J:0,1:N}$ makes sense: in view of our choice of basis functions $\phi_k = w_{k+J}$, its (k,j) element is the numerical approximation to $(\mathcal{R}^0_{\lambda_0} w_k, w_{j+J})_\Gamma$.

The convergence acceleration trick can be repeated if one is prepared to evaluate the matrix elements $R_{k\ell}$ numerically for several different λ. However for the numerical examples which we examined here, one application was always sufficient.

Example 1: Twisted waveguide

We consider the Laplacian in a waveguide in $\mathbb{R}^2$ of width 1, bent through an angle $\pi/4$ as indicated in Fig. 3 (the inner radius of curvature of the bend is 1, the outer radius 2). On the side of the waveguide with the smaller radius of curvature on the bend, Dirichlet conditions are imposed; on the other side the boundary conditions are of Neumann type.

We know that the essential spectrum is determined by the spectrum of the problem on the cylindrical ends only, and is therefore the same as for the unbent waveguide:

$$\sigma_{\rm ess} = [\pi^2/4, +\infty).$$

It may also be shown that for the unbent waveguide the spectrum is purely absolutely continuous. However this changes when the waveguide is bent. Exner et al. [ExSe, DuEx, KrKr] show that bending the waveguide in the direction of the Dirichlet boundary condition will cause an eigenvalue to appear below the essential spectrum. Using the method described in section 14, this eigenvalue can be located quite precisely. For this purpose the inner domain Ω_0 is taken to be the part of the domain between the two dashed lines in Fig. 3. The basis on the cut-off boundary Γ of Ω_0 (the part of $\partial\Omega_0$ composed of the two dashed lines in Fig. 3) is defined as follows. Let s be the local transverse coordinate on Γ measured with $s = 0$ on the 'Dirichlet' side. We denote by ϕ_{2j+1}, $j = 0, 1, 2, \ldots$, the basis functions supported on the vertical portion

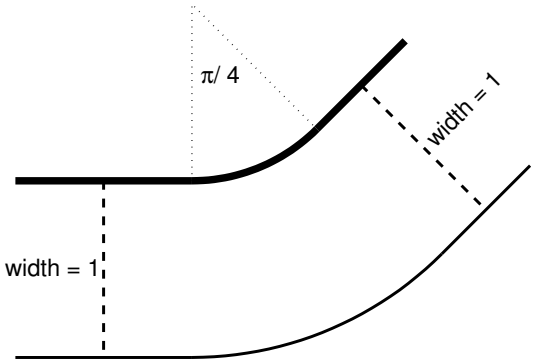

Figure 3: Twisted Waveguide

of Γ, and by ϕ_{2j}, $j = 1, 2, \ldots$, the basis supported on the part of Γ which is at angle $\pi/4$ to the horizontal. In particular, ϕ_{2j} is zero on the vertical part of Γ and ϕ_{2j+1} is zero on the part of Γ which is at angle $\pi/4$ to the horizontal. On their supports, the ϕ_j are given by

$$\phi_j(s) = \begin{cases} \sin(j\pi s/2) & (j \text{ odd}), \\ \sin((j-1)\pi s/2) & (j \text{ even}). \end{cases}$$

Table 1 shows the results of computations at four different levels of accuracy.

Accuracy	Eigenvalue found
silly — 1 mesh refinement; sum over $\lambda_j \leq 10$ in (11.4)	none found
low — 3 mesh refinements; sum over $\lambda_j \leq 50$ in (11.4)	2.3461
medium — 4 mesh refinements; sum over $\lambda_j \leq 100$ in (11.4)	2.3459
high — 5 mesh refinements; sum over $\lambda_j \leq 200$ in (11.4)	2.3454

Table 1: Levels of accuracy and eigenvalue found below the essential spectrum, caused by bending the waveguide.

15 Generalization to resonances

The algorithm of section 14 can be generalized to the calculation of resonances. There are two steps in this generalization.

Firstly, resonances are generally complex. (When a resonance becomes real, it usually becomes either an imbedded eigenvalue, which we have already discussed, or a point of spectral concentration — a local maximum of the derivative of one of the spectral measures associated with the operator.) Since resonances are complex, the condition $\lambda \in [\kappa_J, \kappa_{J+1})$ introduced in

section 9 for the calculation of imbedded eigenvalues no longer makes sense. Of course the equation $-\Delta V = \lambda V$ can still be solved in the cylindrical ends, following the procedure of section 9, and the solution expressed in the form

$$V(x,\mathbf{y}) = \sum_{j=1}^{\infty} c_j(x) w_j(\mathbf{y}).$$

The functions c_j are now chosen to be

$$c_j(x) = c_j^+(x) = -\frac{(g,w_j)}{\sqrt{\kappa_j - \lambda}} \exp\left((x-1)\sqrt{\kappa_j - \lambda}\right).$$

(cf. (9.2)). The reason for such a choice is that for calculation of resonances we drop the condition $V \in H^1_*(\mathcal{C})$ and we explicitly choose the branch of the square root such that $c_j \notin L_2(0,\infty)$. Thus, if we seek resonances (for definiteness, in the lower half-plane $\operatorname{Im}\lambda < 0$), we choose the branch of the square root such that $\operatorname{Re}(\sqrt{\kappa_j - \lambda}) > 0$.

The expression (9.3) remains formally unchanged: however one must choose the branch of the square root as above. A similar remark applies to the matrix T defined in (12.5). With this proviso the matrix pencil (14.5) is formally unchanged, though J must be assigned the value 0.

With these modifications, the resonance approximations are the values of λ such that some σ-eigenvalue $\sigma_j(\lambda)$ of the pencil (14.5) satisfies $\sigma_j(\lambda) = 1$. However calculating the resonances in this way is impractical. Even if the σ_j are analytic functions of λ, which is not guaranteed, it is difficult to order the numerically calculated values of the σ_j to correspond to an analytic ordering.

The simple approach which we used here was to calculate the condition number of the pencil

$$\left[\mathsf{R}^0_{1:M,1:M} + \mathsf{S}_{1:M,1:N}\left\{\mathsf{D}_{1:N,1:N}(\lambda) - \mathsf{D}_{1:N,1:N}(\lambda_0)\right\}(\mathsf{S}_{1:M,1:N})^*\right] - \mathsf{T}_{1:M,1:M}(\lambda). \tag{15.1}$$

as a function of λ and make a contour plot. Local maxima are 'suspicious points' as the condition number will be infinite at a resonance. (The converse, however, is not true: not all local maxima are resonances.) Once suspicious points are located approximately one can 'zoom in' and examine them in more detail.

Example 2: obstructed waveguide

This problem is considered in detail by Aslanyan, Parnovski and Vassiliev [AsPaVa]: a waveguide in $\mathbb{R}^2$ in the strip $|y| < 1$, obstructed by a plane obstacle $\mathcal{O}$ — see Fig. 4. For the particular experiments here, we consider an obstacle which is symmetric about the y-axis. The domain can then be reduced to the strip

$$\{(x,y) \in \mathbb{R}^2 \ : \ x > 0, \ |y| < 1\} \setminus \overline{\mathcal{O}}.$$

Following Aslanyan et al. we take as the obstacle a disc of centre $(0,\delta)$ and radius R, with $|\delta| + R < 1$:

$$\mathcal{O} = \{(x,y) \ : \ x^2 + (y-\delta)^2 < R^2\}.$$

When $\delta = 0$ the problem has an eigenvalue imbedded in the essential spectrum. When δ is perturbed from zero, the eigenvalue evolves into a resonance, analytically as a function of δ (see

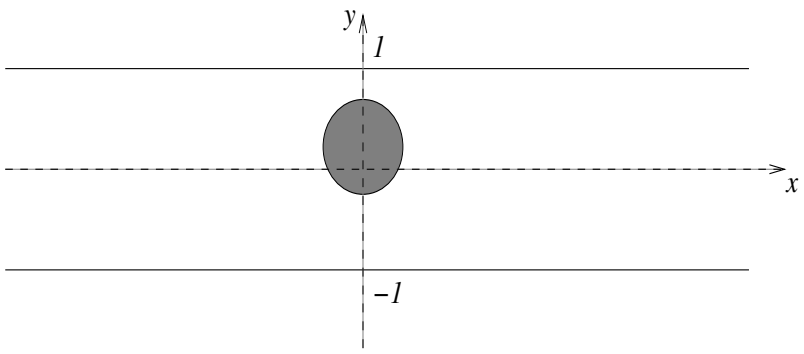

Figure 4: Waveguide obstructed by an obstacle

[AsPaVa]). For the numerical experiments we truncated the strip at $x = 1$: thus, we took as our domain Ω_0 the set

$$\{(x, y) \in \mathbb{R}^2 \,:\, 0 < x < 1,\ |y| < 1\} \setminus \overline{\mathcal{O}}.$$

Table 2 shows the results for various values of the numerical experiment parameters. Each is quoted for four 'levels of accuracy' defined in Table 1.

δ	R=0.3	R=0.5
0.0	1.50866 (silly) 1.50499 (low acc.) 1.50489 (medium acc.) 1.50486 (high acc.) 1.5048 (Aslanyan et al.)	1.39806 (silly) 1.39157 (low acc.) 1.39139 (medium acc.) 1.39134 (high acc.) 1.3913 (Aslanyan et al.)
0.1	$1.5120 + 10^{-4}i$ (silly) $1.5080 + 10^{-4}i$ (low acc.) $1.5079 + 10^{-4}i$ (medium acc.) $1.5078 + 10^{-4}i$ (high acc.) $1.5102 + 10^{-4}i$ (Aslanyan et al.)	$1.4043 + 8 \times 10^{-4}i$ (silly) $1.3981 + 9 \times 10^{-4}i$ (low acc.) $1.3979 + 9 \times 10^{-4}i$ (medium acc.) $1.3979 + 9 \times 10^{-4}i$ (high acc.) $1.3998 + 9 \times 10^{-4}i$ (Aslanyan et al.)
0.2	$1.5203 + 4 \times 10^{-4}i$ (silly) $1.5167 + 5 \times 10^{-4}i$ (low acc.) $1.5165 + 5 \times 10^{-4}i$ (medium acc.) $1.5165 + 5 \times 10^{-4}i$ (high acc.) $1.5188 + 5 \times 10^{-4}i$ (Aslanyan et al.)	$1.4236 + 3.46 \times 10^{-3}i$ (silly) $1.4180 + 3.89 \times 10^{-3}i$ (low acc.) $1.4178 + 3.89 \times 10^{-3}i$ (medium acc.) $1.4178 + 3.90 \times 10^{-3}i$ (high acc.) $1.4196 + 3.93 \times 10^{-3}i$ (Aslanyan et al.)

Table 2: Experiments on the obstructed waveguide.

The agreement with the results of Aslanyan et al. is good for the case of obstacle displacement $\delta = 0$ (the case of an embedded eigenvalue). In the cases $\delta > 0$ the agreement is less good, but the error is no worse than 2×10^{-3}. The values which we calculate change very little between the medium and high accuracy cases.

16 Generalizations — resonances of a scatterer

In section 15 we described how to calculate resonances in the case when the domain has cylindrical ends. In fact a similar approach can be used to calculate resonances due to scattering by an obstacle. We consider a situation similar to that in Fig. 5, in which the domain is the region exterior to an obstacle (the shaded region). The cylindrical ends are now replaced by the region $x^2+y^2>R^2$ and the boundary Γ is the circle of centre $(0,0)$, radius R.

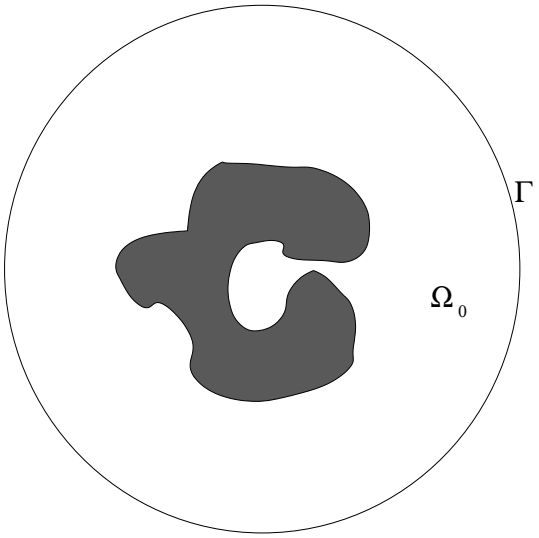

Figure 5: Scattering by an obstacle. The transverse boundary Γ is replaced by a circle of radius R, the cylindrical ends by the region $x^2+y^2>R^2$.

As in section 15, we can compute resonances by replacing the map $\mathcal{R}^{\mathcal{C}}_{\lambda}$ of (9.3) by the appropriate Neumann to Dirichlet map for the exterior region. A simple separation of variables shows that, in terms of appropriate Hankel functions H_n,

$$\mathcal{R}^{\mathcal{C}}_{\lambda}g=\frac{1}{\sqrt{2\pi}}\sum_{n\in\mathbb{Z}}g_n\frac{H_n(R\sqrt{\lambda})}{\sqrt{\lambda}H_n'(R\sqrt{\lambda})}\mathrm{e}^{in\theta}, \tag{16.1}$$

in which the Fourier coefficients g_n are

$$g_n=\frac{1}{\sqrt{2\pi}}\int_0^{2\pi}g(\phi)\mathrm{e}^{-in\phi}\mathrm{d}\phi.$$

Suppose that we are interested in resonances which lie in the half-plane $\mathrm{Im}(\lambda)<0$. Then choosing the branch of the square root so that $\mathrm{Im}(\sqrt{\lambda})<0$, the required Hankel functions are the ones which grow as

$$H_n(r\sqrt{\lambda})\sim r^{-1/2}\mathrm{e}^{-r\,\mathrm{Im}\,\sqrt{\lambda}}, \tag{16.2}$$

as $r\to+\infty$. These are the Hankel functions of the first kind.

The matrix T of (12.5) is now replaced by a matrix which is clearly still diagonal. If we order the functions $\{\mathrm{e}^{in\theta} \,|\, n \in \mathbb{Z}\}$ in the order

$$\{1, \mathrm{e}^{i\theta}, \mathrm{e}^{-i\theta}, \mathrm{e}^{2i\theta}, \mathrm{e}^{-2i\theta}, \ldots\}$$

then the corresponding matrix T is

(16.3)

$$\mathsf{T} = \mathrm{diag}\left(\frac{H_0(R\sqrt{\lambda})}{\sqrt{\lambda}H_0'(R\sqrt{\lambda})}, \frac{H_1(R\sqrt{\lambda})}{\sqrt{\lambda}H_1'(R\sqrt{\lambda})}, \frac{H_{-1}(R\sqrt{\lambda})}{\sqrt{\lambda}H_{-1}'(R\sqrt{\lambda})}, \frac{H_2(R\sqrt{\lambda})}{\sqrt{\lambda}H_2'(R\sqrt{\lambda})}, \frac{H_{-2}(R\sqrt{\lambda})}{\sqrt{\lambda}H_{-2}'(R\sqrt{\lambda})}, \ldots \right).$$

The resonances can then be calculated following the same procedure as in section 15.

Example 3: a cavity resonance problem

We consider scattering by a C-shaped barrier almost enclosing a cavity as shown in Fig. 6.

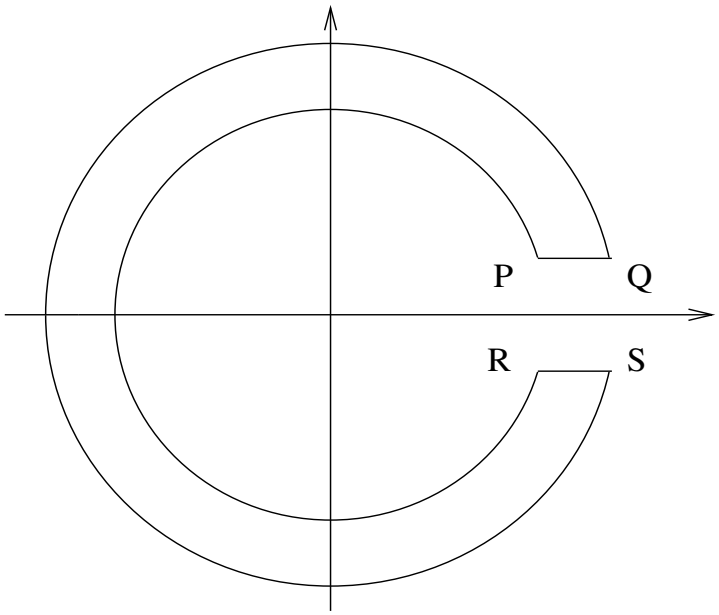

Figure 6: Cavity Resonator. The points P, Q, R and S have coordinates $(1, \epsilon)$, $(1.1, \epsilon)$, $(1.1, -\epsilon)$ and $(1, -\epsilon)$ respectively, and are joined by two circular arcs

On the boundary of the domain we impose Dirichlet boundary conditions. For the Laplacian on this domain, $\sigma_{ess} = [0, +\infty)$. By simple separation of variables it is easy to show that no non-trivial solution of the Poisson equation $-\Delta u = \lambda u$ on this exterior domain can lie in L_2 for $\lambda \geq 0$, no matter what boundary conditions it may satisfy. Thus there can be no embedded eigenvalues.

Nevertheless it is known (see [BroHiMa]) that for small ϵ this problem possesses a resonance close to each Dirichlet eigenvalue for the Laplacian on the unit disc. We wish to compute these resonances.

We first create an 'inner domain' by introducing an artificial outer boundary which is a circle centred at the origin with radius $R > 1.1$. It is important that R not be too large: as $R \to \infty$, the (Neumann and Dirichlet) eigenvalues of the inner domain become dense in any compact subset of $[0, \infty)$, and so in particular it becomes very difficult to distinguish resonances close to the real axis from Neumann eigenvalues of the inner domain. For numerical reasons it is's also important that R not be too close to 1.1: otherwise the annular region $1.1 < \sqrt{x^2+y^2} < R$ becomes very narrow, requiring a very fine mesh, and the numerical calculations require too much computing time. We carried out our calculations for $R = 1.3$ and, as a check, for $R = 1.5$.

The Dirichlet problem on the unit disc has eigenvalues 5.783 (simple) and 14.682 (multiplicity 2). We started by calculating the first channel resonances of the C-shape resonator closest to these eigenvalues. The results are shown in Table 3. The resonance closest to the first of these

	$\epsilon = 0.2$	$\epsilon = 0.3$
Medium Accuracy	$5.5158 - 4.8 \times 10^{-4} i$	$5.1987 - 4.9 \times 10^{-3} i$
	$13.8574 - 4 \times 10^{-4} i$	$12.7505 - 0.1045 i$
High Accuracy	$5.5141 - 4.6 \times 10^{-4} i$	$5.1976 - 5.1 \times 10^{-3} i$
	$13.8554 - 9.7 \times 10^{-3} i$	$12.8165 - 0.1025 i$

Table 3: Resonance calculations for C-shaped resonator. Levels of accuracy: 'medium' means 4 mesh refinements, $R = 1.5$ and $\lambda_{\mathsf{max}} = 50$; 'high' means 5 mesh refinements, $R = 1.3$ and $\lambda_{\mathsf{max}} = 100$.

eigenvalues is rather difficult to calculate accurately because it is so close to a pole of $\mathcal{R}^0_\lambda$, the Neumann-Dirichlet map of the interior domain whose poles are the Neumann eigenvalues of the interior domain. See Fig. 7, which shows a contour plot of

$$\left|\det(L_{\mathsf{inner}}(\lambda) L^{-1}_{\mathsf{outer}}(\lambda) - I)\right|,$$

where, in view of (15.1), L_{inner} is given by

$$L_{\mathsf{inner}}(\lambda) = \mathsf{R}^0_{1:M,1:M} + \mathsf{S}_{1:M,1:N} \left\{\mathsf{D}_{1:N,1:N}(\lambda) - \mathsf{D}_{1:N,1:N}(\lambda_0)\right\} (\mathsf{S}_{1:M,1:N})^*,$$

while $L_{\mathsf{outer}}(\lambda)$ is the analytic continuation of $\mathsf{T}_{1:M,1:M}(\lambda)$ already described. The point close to $5.2 - 5 \times 10^{-3} i$ is the zero of the determinant, and is the approximate resonance. It is not easy to see this zero so close to the nearby pole. This requires sampling of the determinant on a very fine grid, which is expensive.

The resonance close to the second eigenvalue is not so close as to cause the same numerical difficulties.

We also sought to calculate resonances further out in the complex plane. These are rather more difficult to obtain - see Fig. 8, where we compare the results for the medium and high levels of accuracy. The agreement is rather poor. In fact the change in R is more responsible for this than the level of mesh refinement or the value of λ_{max} for fixed R. This is rather different from the situation in [Ma], where the resonances were calculated by complex scaling. There, the sensitive resonances depended more on the mesh than on the domain of truncation.

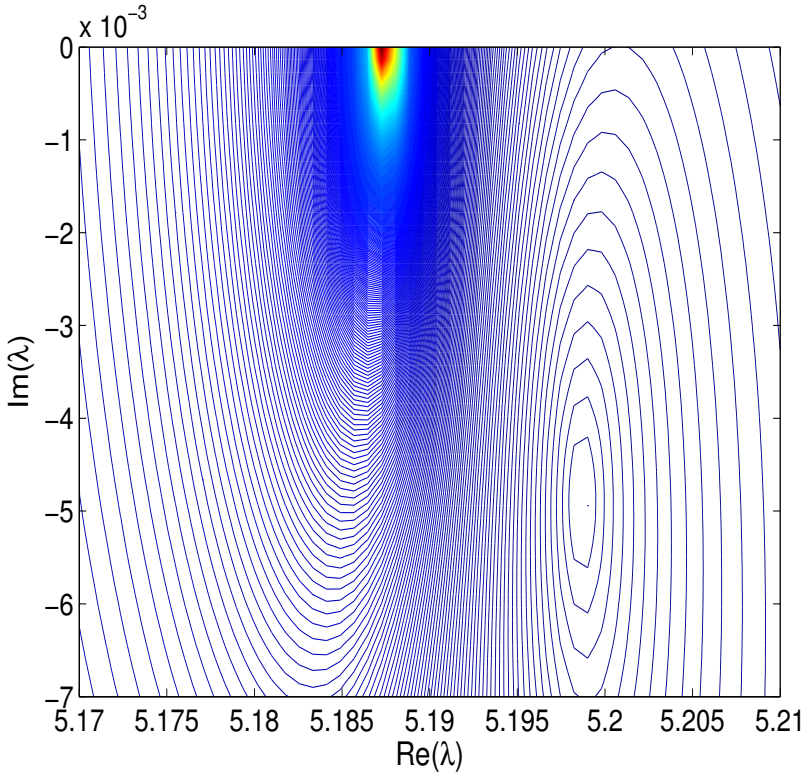

Figure 7: Resonance very close to a Neumann eigenvalue for the interior domain; $R = 1.5$, $\epsilon = 0.3$. At lower resolutions these are virtually indistinguishable. This is a problem, as not all Neumann eigenvalues are close to resonances! The contours are the level sets of a determinant which is zero at the resonance $5.199 - 5 \times 10^{-3} i$. Unfortunately the same determinant also has a pole at the nearby Neumann eigenvalue 5.187.

Example 4: Scattering by a Gaussian potential

We consider the resonances of the Schrödinger operator in $L_2(\mathbb{R}^2)$ given by $-\Delta + q(x,y)$ where q is a superposition of three Gaussians:

$$q(x,y) = C \sum_{j=1}^{3} \exp(-\nu(x-x_j)^2 - \nu(y-y_j)^2),$$

with $(x_1, y_1) = (0, -1)$, $(x_2, y_2) = (\sin(\pi/3), \cos(\pi/3))$, $(x_3, y_3) = (-x_2, y_2)$, $C = 40$ and $\nu = 2$. For large C there is a high potential barrier on the unit circle $x^2 + y^2 = 1$ which gives rise to almost-trapped modes. However because q is rapidly decaying the PDE $-\Delta u + qu = \lambda u$ in fact has no non-trivial L_2 solutions for $\lambda \geq 0$. The almost-trapped modes are the real parts of resonances close to the real axis, which one may attempt to compute by the same approach as for Example 3.

An inner domain is created with boundary on the circle $x^2 + y^2 = R^2$. The value of R should be chosen so that for $x^2 + y^2 > R^2$, the function q is small enough to be neglected,

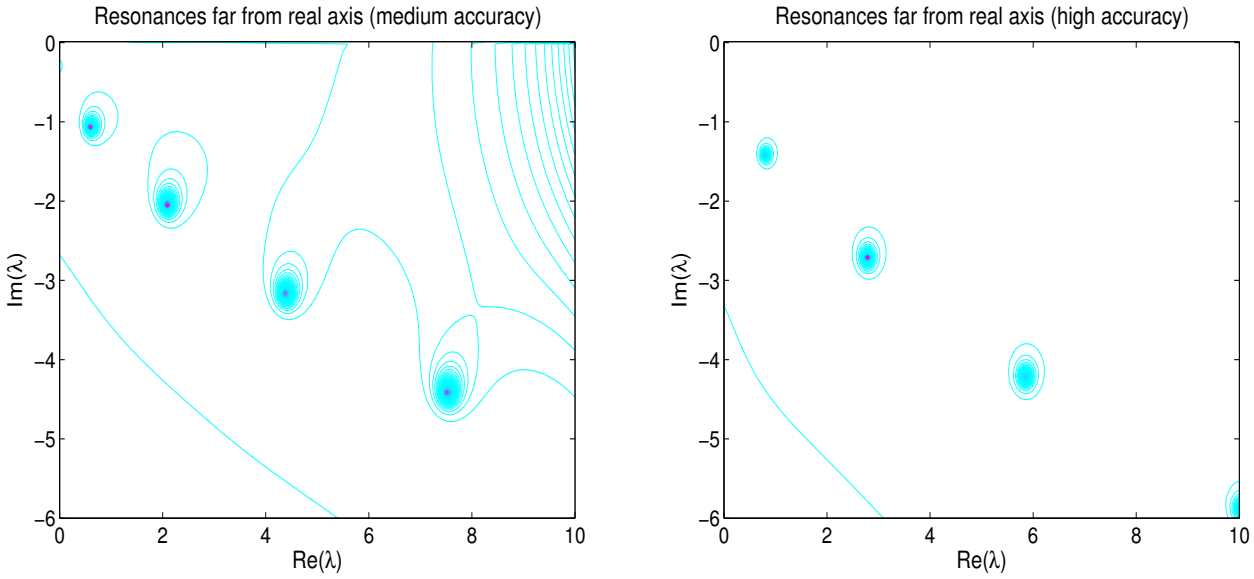

Figure 8: Resonances far from the real axis for $\epsilon = 0.2$: the medium and high accuracy results are only qualitatively similar

which allows the PDE to be approximated by the Helmholtz equation. This allows us to use the same expression for the outer Neumann-Dirichlet map as for Example 3.

As for Example 3, resonances far from the real axis are very unstable and cannot be calculated reliably. However we were able to calculate some resonances close to the real axis with moderate accuracy. One case is listed in Table 4.

$\lambda_{\max}$	No. of mesh refines	R	Resonance
50	2	4.0	$4.257 - 5 \times 10^{-4} i$
50	3	4.0	$4.140 - 5 \times 10^{-4} i$
50	3	5.0	$4.185 - 10^{-3} i$
50	4	6.0	$4.402 - 4 \times 10^{-4} i$

Table 4: Resonance calculations for Gaussian potential.

Lin [Li] attempts to find these resonances using the complex scaling method and a specially developed variational PDE-solver with a particularly chosen set of basis functions. Even then, many spurious results are generated, and Lin claims to be able to filter them out.

17 Conclusions

Although our original motivation for doing this work lay in the need to devise a numerical method which would be easy to implement, the numerical results show that the accuracy achieved by our approach is actually quite competitive with conventional techniques. Moreover, although Neumann series converge rather slowly, two features ensure that for these problems the run-

times were not excessive: firstly, the fact that the quantities in the eqn. (12.2) are calculated once at the outset, so the most expensive calculations need not be repeated for each different λ at which the Neumann-Dirichlet maps are evaluated; secondly, the trick in eqn. (14.4) acts as a convergence acceleration technique for the Neumann expansion and means that in many cases we are able to get away with very few eigenfunctions.

There are further modifications which could easily be made to improve efficiency. Foremost among these would be to replace contour-plotting of the condition number $\kappa(R(\lambda)+T(\lambda))$ by a routine based on contour integration for finding zeros of an analytic function. There are good practical reasons, however, for not doing this. Resonances close to the real axis can already be located quite accurately by finding the maxima, along the real axis, of $\kappa(R(\lambda)+T(\lambda))$; this is easy since it is a one-dimensional search. As already observed by Abramov, Aslanyan and Davies [AbAsDa], resonances further from the real axis are typically very unstable; to spend a lot of time accurately locating the resonances of an approximating problem is therefore pointless.

References

[AbAsDa] A. A. Abramov, A. Aslanyan, and E. B. Davies, *Bounds on complex eigenvalues and resonances*. J. Phys. A **34**, 57–72 (2001).

[Ag] M. S. Agranovich, *Poincaré–Steklov type operators in domains with Lipschitz boundaries*. Lecture presented at Durham/LMS Symposium on 'Operator Theory and Spectral Analysis', August 2005. `www.maths.dur.ac.uk/events/Meetings/LMS/2005/OTSA/Talks/agranovich.pdf`.

[AsPaVa] A. Aslanyan, L. Parnovski, and D. Vassiliev, *Complex resonances in acoustic waveguides*. Q. Jl. Mech. Appl. Math. **53**, 429-447 (2000).

[BoJo] A.-S. Bonnet-Ben Dhia and P. Joly, *Mathematical analysis of guided water waves*. SIAM J. Appl. Math. **53**, no. 6, 1507–1550 (1993).

[Bo] A. Boumenir, *The impedance tomography problem*. Proc. Amer. Math. Soc. **131**, no. 11, 3553–3557 (2003) (electronic).

[BreTeWr] C. A. Brebbia, J. C. F. Telles, and L. C. Wrobel, *Boundary Element Techniques*. Springer-Verlag, Berlin, 1984.

[BroHiMa] R. M. Brown, P. D. Hislop, and A. Martinez, *Lower bounds on the interaction between cavities connected by a thin tube*. Duke Math. J. **73**, no. 1, 163–176 (1994).

[Ch] T. Christiansen, *Scattering theory for manifolds with asymptotically cylindrical ends*. J. Funct. Anal. **131**, no. 2, 499–530 (1995).

[ChZw] T. Christiansen and M. Zworski, *Spectral asymptotics for manifolds with cylindrical ends*. Ann. Inst. Fourier (Grenoble) **45**, no. 1, 251–263 (1995).

[CoKr] D. Colton and R. Kress, *Integral equation methods in scattering theory*. John Wiley, N.Y., 1983.

[DaPa] E. B. Davies and L. Parnovski, *Trapped modes in acoustic waveguides*. Q. Jl. Mech. Appl. Math. **51**, 477–492 (1998).

[DuEx] P. Duclos and P. Exner, *Curvature-induced bound states in quantum waveguides in two and three dimensions*. Rev. Math. Phys. **7**, 73–102 (1995).

[EvLeVa] D. V. Evans, M. Levitin, and D. Vassiliev, *Existence theorems for trapped modes*. J. Fluid Mech. **261**, 21–31 (1994).

[ExSe] P. Exner and P. Šeba, *Bound states in curved quantum waveguides*. J. Math. Phys. **30**, 2574–2580 (1989).

[Fr] L. Friedlander, *Some inequalities between Dirichlet and Neumann eigenvalues*. Arch. Rat. Mech. Anal. **116**, 153–160 (1991).

[GiPaKe] D. Givoli, I. Patlashenko and J. B. Keller, *Discrete Dirichlet to Neumann maps for unbounded domains*. Comput. Methods Appl. Mech. Engrg. **164**, 173-185 (1998).

[HaPaGi] I. Harari, I. Patlashenko, and D. Givoli, *Dirichlet-to-Neumann maps for unbounded wave guides*. J. Comput. Phys. **143**, no. 1, 200–223 (1998).

[HaKe] T. Hägstrom and H. B. Keller, *Asymptotic boundary conditions and numerical methods for nonlinear elliptic problems on unbounded domains*. Math. Comp. **48**, 449–470 (1970).

[KrKr] D. Krejčiřík and J. Kříž, *On the spectrum of curved quantum waveguides*. Publ. RIMS, Kyoto University **41**, no. 3., 757–791 (2005).

[Li] K. K. Lin, *Numerical study of quantum resonances in chaotic scattering*. J. Comput. Phys. **176**, no. 2, 295–329 (2002).

[Ma] M. Marletta, *Eigenvalue problems on exterior domains and Dirichlet to Neumann maps*. J. Comput. Appl. Math. **171**, no. 1-2, 367–391 (2004).

[McILiMcIZh] M. McIver, C. M. Linton, P. McIver, and J. Zhang, *Embedded trapped modes for obstacles in two-dimensional waveguides*. Q. Jl. Mech. Appl. Math. **54**, 273–293 (2001).

[Pal] V.B. Pal'tsev, *On a mixed problem with nonhomogeneous boundary conditions for second order elliptic equations with a parameter in Lipschitz domains*. Sb. Math. **187**, no. 4, 525–580 (1996).

[Par] L.B. Parnovski, *Spectral asymptotics of the Laplace operator on manifolds with cylindrical ends*. Internat. J. Math. **6**, no. 6, 911–920 (1995).

[PeJo] D. Gómez Pedreira and P. Joly, *A method for computing guided waves in integrated optics. I. Mathematical analysis*. SIAM J. Numer. Anal. **39**, no. 2, 596–623 (2001) (electronic); *II. Numerical approximation and error analysis*. SIAM J. Numer. Anal. **39**, no. 5, 1684–1711 (2001/02) (electronic).

[Sa] Yu. Safarov, *Dirichlet-to-Neumann operator for nonsmooth boundaries*. Preprint, 2005.

[Ur] F. Ursell, *Mathematical aspects of trapping modes in the theory of surface waves*. J. Fluid Mech. **183**, 421–437 (1987).